Faraday Discussions

Cite this: *Faraday Discuss.*, 2015, **178**, 335

ROYAL SOCIETY OF CHEMISTRY

PAPER

View Article Online
View Journal | View Issue

Published on 18 November 2014. Downloaded by UNIVERSIDAD DE ZARAGOZA on 11/06/2015 13:47:58.

Nonlinear quantum optics in the (ultra) strong light–matter coupling

Eduardo Sánchez-Burillo,[a] Juanjo García-Ripoll,[b] Luis Martín-Moreno[a] and David Zueco[ac]

Received 16th October 2014, Accepted 20th October 2014
DOI: 10.1039/c4fd00206g

The propagation of N photons in one dimensional waveguides coupled to M qubits is discussed, both in the strong and ultrastrong qubit–waveguide coupling. Special emphasis is placed on the characterisation of the nonlinear response and its linear limit for the scattered photons as a function of N, M, qubit inter distance and light–matter coupling. The quantum evolution is numerically solved *via* the matrix product states technique. The time evolutions for both the field and qubits are computed. The nonlinear character (as a function of N/M) depends on the computed observable. While perfect reflection is obtained for $N/M \cong 1$, photon–photon correlations are still resolved for ratios $N/M =$ non-zero. Inter-qubit distance enhances the nonlinear response. Moving to the ultrastrong coupling regime, we observe that inelastic processes are robust against the number of qubits and that the qubit–qubit interaction mediated by the photons is qualitatively modified. The theory developed in this work models experiments in circuit QED, photonic crystals and dielectric waveguides.

1 Introduction

Typically, materials respond linearly to an electromagnetic (EM) field. Intense fields are usually demanded for accessing nonlinear responses.[1] Therefore, a long standing challenge in science and technology is to develop devices containing giant nonlinear properties that operate at small powers. The final goal is to shrink the required power to the few photon limit.[2,3] In doing so, the dipoles must interact more strongly with the driving photons than with the environment, which defines the strong light–matter coupling regime. Thus, quantum optical systems presenting strong light–matter interactions are excellent candidates for building nonlinear optical materials operating at tiny powers.

An ideal platform for having strong light–dipole coupling together with the possibility of generating and measuring few photon currents is waveguide QED.

[a]*Instituto de Ciencia de Materiales de Aragón y Departamento de Física de la Materia Condensada, CSIC-Universidad de Zaragoza, Zaragoza, E-50009, Spain*
[b]*Instituto de Física Fundamental, IFF-CSIC, Serrano 113-bis, Madrid E-28006, Spain*
[c]*Fundación ARAID, Paseo María Agustín 36, Zaragoza 50004, Spain*

Published on 18 November 2014. Downloaded by UNIVERSIDAD DE ZARAGOZA on 11/06/2015 13:47:58.

There, the paradigmatic dipoles are two level systems (qubits) and the input and output fields travel through one dimensional waveguides. As there are only two propagation directions (left and right), interference effects are much larger than in 3D. Besides, the coupling to the qubits is enhanced by the reduced dimensionality (the Purcell effect). Different platforms can serve for the study: circuit-QED,[4–7] quantum dots interacting with photonic crystals,[8] dielectric waveguides,[9] molecules interacting with photons[10] or plasmonic devices.[11–15] With this kind of systems different nonlinear effects may be observed and used, such as photon–photon correlations,[16–30] non-classical light generation,[31] lasing[32] or effective interaction between noninteracting dipoles.[33–37]

Light–matter coupling, even when it is larger than the losses, is typically much smaller than the characteristic energy scales of qubits (dipoles) and photons. In this case, up to second order in this coupling, only processes where light and matter exchange excitations play a role. This is the Rotating Wave Approximation (RWA).[38] Quite recently, experiments have reached couplings large enough for this approximation to break down.[39–42] Then, the full dipole interaction must be taken into account and, in order to understand the experiments, it is indispensable to consider processes involving the spontaneous creation and annihilation of pairs of excitations. This is the ultrastrong coupling regime. Beyond the RWA picture novel physics has been predicted,[43–47] also from the scattering point of view.[48,49] Clearly, this regime has a great potential for nonlinear applications.

It is desirable to quantify the amount of nonlinearity for a given architecture with a given input driving, like in classical nonlinear optics, where materials are classified *via* their linear and nonlinear susceptibilities. Furthermore, some systems can behave as linear when looking at one quantity and nonlinear when measuring another. In general, the response is expected to be linear in the low polarisation limit, $N/M \ll 1$, with N the number of photons and M the number of qubits. In this work, we quantify more precisely this linear–nonlinear transition. In doing so, we must acknowledge that the description of qubits and currents containing few photons needs a quantum treatment. To compute this quantum evolution, we choose the Matrix Product State (MPS) technique adapted for photonic situations.[46,48] Within the MPS, the exact dynamics is computed for multiphoton input states passing through several qubits both in the strong and ultrastrong coupling regimes. We explore the dynamics by changing the ratio N/M and the light–matter coupling strength. Our aim here is to discuss the tradeoff between the enhancement of the coupling with the number of qubits (which, accordingly to the theory of Dicke states[50] scales as $g\sqrt{M}$) at the expense of decreasing the nonlinear response. Besides this, we also study the influence of the distance between the dipoles. Finally, we will explore the changes on this RWA phenomenology when moving to the ultrastrong coupling regime. As witnesses for the nonlinearities we will compute transmission and reflection probabilities, qubit populations and photon–photon correlations.

The rest of this discussions is organised as follows. Section 2 summarises the theoretical basis needed for understanding the results. Section 3 discusses the analytic properties for the scattering matrix in linear systems (*i.e.* when the scatterers are harmonic resonators), linking the notion of linear quantum system with linear optical response. The numerical results both in the RWA and beyond

 This journal is © The Royal Society of Chemistry 2015

Published on 18 November 2014. Downloaded by UNIVERSIDAD DE ZARAGOZA on 11/06/2015 13:47:58.

the RWA are presented in Sections 4 and 5 respectively. Our conclusions and two technical Appendices close the paper.

2 Theoretical background

In this section we summarise the quantum theory for scattering in waveguide QED. We also outline the MPS technique used in our numerical simulations.

2.1 Physical setup

This work deals with the dynamics of photons moving in a one dimensional waveguide interacting with a discrete number of dipoles. A pictorial representation is given in Fig. 1a. The waveguide is discretised and the quantum dipoles (scatterers) are point-like systems interacting with the photons accordingly to the dipole approximation, $H_{\rm int} \propto \mathbf{E}\cdot\mathbf{p}$. The Hamiltonian is,

$$H_{\rm tot} = \varepsilon \sum_x a_x^\dagger a_x - J \sum_x \left(a_x^\dagger a_{x+1} + hc\right) + \sum_{i=1}^{M} \left(h_i\left(c_i, c_i^\dagger\right) + g_i\left(c_i + c_i^\dagger\right)\left(a_{x_i} + a_{x_i}^\dagger\right)\right). \tag{1}$$

Here, the waveguide is modeled within the first two terms. It is an array of $N_{\rm cav} = 2L + 1$ coupled cavities, running x from $-L$ to L, with bare frequencies ε and hopping between nearest neighbours J. The photon operators satisfy bosonic relations $[a_x, a_{x'}^\dagger] = \delta_{xx'}$. The free propagation is characterised by a cosine-shaped

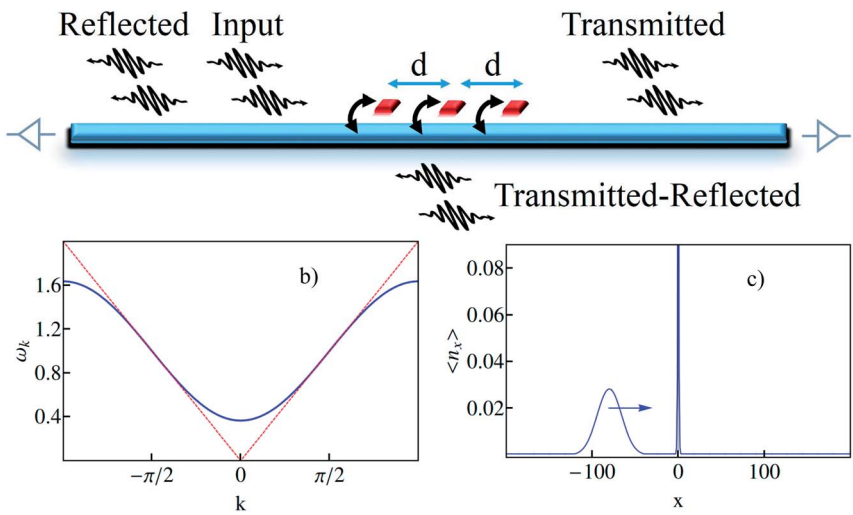

Fig. 1 (a) Schematic representation of the system: waveguide with input and output fields and the qubits (red squares) separated by a distance d. (b) Dispersion relation (blue curve) for $\varepsilon = 1$ and $J = 1/\pi$ and 400 cavities (these parameters will be used throughout the text). The dashed red line is the linearisation of ω_k around $k = \pi/2$. (c) Computed number of photons as a function of position in the chain (14) for an incident wavepacket ($N = 1$) impinging on one qubit ($\Delta = 1$) taking the full interaction Hamiltonian (1) with $g = 0.7$. There is a photonic cloud around the qubit position ($x = 0$), corresponding to the ground state. This ground state was computed with the MPS method, as explained in Section 2.3.

Published on 18 November 2014. Downloaded by UNIVERSIDAD DE ZARAGOZA on 11/06/2015 13:47:58.

dispersion relation $\omega_k = \varepsilon - 2J\cos k$, as shown in Fig. 1(b). Under some circumstances and working in the middle of the band $k \cong \pi/2$, the linearised dispersion $\omega_k = \nu k$ with $\nu = 2J$ is well justified. Such a linearisation is not performed in our numerical investigations, but it can be important to have it in mind when comparing some of our findings with analytical treatments (mostly done with linear dispersion relations). The dipoles are characterised *via* the ladder operators $c_i^\dagger$ (c_i). In the numerical work presented in this paper, we will consider qubits,

$$c_i^\dagger = \sigma_i^+, \text{ with, } [\sigma_i^+,\sigma_j^-] = \delta_{ij}\,(2\sigma_i^+\sigma_i^- - 1) \tag{2}$$

and

$$h_i\,(c_i,c_i^\dagger) = \Delta_i c_i^\dagger c_i \tag{3}$$

with Δ_i the frequency for each qubit. Other nonlinear dipoles could be investigated without extra difficulty *e.g.* three level atoms[51,52] or Kerr-type punctual materials.[30] We can also consider linear dipoles, *i.e.*, harmonic oscillators satisfying bosonic commutation relations $[c_i,c_j^\dagger] = \delta_{ij}$, as we will do in Section 3.4 in order to explore the linear limit.

The last term in (1) results from the quantisation of the dipole interaction term $(H_{\text{int}})_i \propto \mathbf{E}(x_i)\cdot\mathbf{p}_i$, because $\mathbf{E}(x_i) \sim a_{xi} + \text{hc}$ (ref. 53) and $p_i \sim c_i^\dagger + \text{hc}$.[38] The coupling strength is given by the constants g_i, whose actual value will depend on the concrete physical realisation. If $g_i \ll \Delta_i$ we can approximate the interaction as,

$$H_{\text{int}} = g\sum_{i=1}^{M}\left(c_i + c_i^\dagger\right)\left(a_{x_i} + a_{x_i}^\dagger\right) \simeq g\sum_{i=1}^{M}\left(c_i^\dagger a_{x_i} + c_i a_{x_i}^\dagger\right) \equiv H_{\text{int}}^{\text{RWA}}. \tag{4}$$

i.e. we have neglected the counter-rotating terms $c_i^\dagger a_{x_i}^\dagger + \text{hc}$. This is the so-called Rotating Wave Approximation (RWA), which is valid up to $\mathcal{O}(g_i^2)$.[38] It is widely used since $g_i \ll \Delta_i$ typically holds in the experiments. Within the RWA, the number of excitations is conserved, $[H,\mathcal{N}] = 0$, with the number operator $\mathcal{N} \equiv \sum_x a_x^\dagger a_x + \sum_i c_i^\dagger c_i$. This symmetry highly reduces the complexity of solving the dynamics of (1).

If g_i is not a small parameter, the RWA is not justified and the full dipole interaction [the last term in (1)] must be taken into account. The regime where the RWA is not sufficient for describing the phenomenology is known as the ultrastrong coupling regime.[39–42] Here, the number of excitations is not conserved, making the problem much harder to solve.

A good example to observe the extra complexity is the computation of the ground state for (1), which is an essential step in the scattering process. Within the RWA, the ground state is trivial, $|\text{GS}\rangle_{\text{RWA}} = |0\rangle$, with $a_x|0\rangle = 0$ for all x and $c_j|0\rangle = 0$ for all j. Beyond the RWA, in the ultrastrong coupling regime, the $|\text{GS}\rangle$ is a correlated state with $\langle\text{GS}|\mathcal{N}|\text{GS}\rangle \neq 0$. In Fig. 1(c) the photon population in the waveguide per site, $\langle n_x\rangle = \langle\Psi|a_x^\dagger a_x|\Psi\rangle$ is plotted, being $|\Psi\rangle$ the ground state with a flying photon (eqn (5) for $N = 1$). There, only one qubit is coupled to the waveguide beyond the RWA ($g = 0.7[\Delta]$). Around the qubit (placed at $x = 0$) a non trivial structure appears. The peaked wavepacket around $x = -90$ is the flying photon.

Published on 18 November 2014. Downloaded by UNIVERSIDAD DE ZARAGOZA on 11/06/2015 13:47:58.

2.2 Scattering

We are interested in computing the scattering characteristics for N-photon input states interacting with M qubits. The input state, our initial condition, is chosen to be the non-normalised quantum state.

$$|\Psi_{\rm in}\rangle = \left(a_\phi^\dagger\right)^N |{\rm GS}\rangle, \quad a_\phi^\dagger = \sum_x \phi_x^{\rm in} a_x^\dagger, \tag{5}$$

where $|{\rm GS}\rangle$ is the ground state of the system [see Fig. 1(c)] and $\phi_x^{\rm in}$ is a Gaussian wavepacket centred in $x_{\rm in}$ with spatial width θ

$$\phi_x^{\rm in} = \exp\left(-\frac{(x-x_{\rm in})^2}{2\theta^2} + ik_{\rm in}x \right). \tag{6}$$

Typically, we consider $x_{\rm in}$ located on the left hand side of the qubits with the wavepacket moving to the right toward the scatterers, as sketched in Fig. 1(a) and computed in Fig. 1(c).

In several scenarios, it will be convenient to work in momentum space,

$$a_k^\dagger = \frac{1}{\sqrt{L}} \sum_x {\rm e}^{ikx} a_x^\dagger. \tag{7}$$

In momentum space the wavepacket (6) is exponentially localised around $k_{\rm in}$, with width $\sim \theta^{-1}$.

In our numerical simulations we evolve the initial state (5) unitarily,

$$|\Psi(t)\rangle = U(t,0)|\Psi_{\rm in}\rangle = {\rm e}^{-iH_{\rm tot}t}|\Psi_{\rm in}\rangle. \tag{8}$$

We stop the simulation at a final time $t_{\rm out}$, which must be sufficiently large for the photons to be moving freely along the waveguide, after having interacted with the scatterers. In doing so, our numerics account for stationary amplitudes encapsulated in the definition of the scattering matrix, S,

$$|\Psi_{\rm out}\rangle = S|\Psi_{\rm in}\rangle. \tag{9}$$

It is customary to specify the scattering matrices through their momentum components:

$$S_{p_1\ldots p_{N'},k_1\ldots k_N} = \langle GS|a_{p_1}\ldots a_{p_{N'}} S a_{k_1}^\dagger \ldots a_{k_N}^\dagger|{\rm GS}\rangle. \tag{10}$$

Some comments are pertinent here. The $|{\rm GS}\rangle$ appears in the definition of S. As discussed before, in the ultrastrong coupling regime the ground state differs from the vacuum state, and has a non-zero number of excitations, see Fig. 1(c). In the ultrastrong regime the number of excitations is not conserved. Therefore, in the above formula $N' \neq N$ in general. The components, $S_{p_1\ldots pN',k_1\ldots kN}$ can be numerically computed as projections of the evolved state as we will explain below.

2.3 Matrix Product States for scattering problems

As previously stated, beyond RWA even the ground state is non trivial. The problem becomes a many-body one and we must consider the full Hilbert space

Published on 18 November 2014. Downloaded by UNIVERSIDAD DE ZARAGOZA on 11/06/2015 13:47:58.

for any computation. If we truncate the number of particles per site to $n_{\max}$ and our scatterers are qubits, the dimension of the Hilbert space is $2^M(n_{\max}+1)^{N_{\text{cav}}}$, which is exponential with both N_{cav} and M. Numerical brute force is impossible and analytical tools are really limited. Even within the RWA, if we work with N photons and M qubits the Hilbert space dimension, $(N_{\text{cav}}+M)^N$, is also too large for multiphoton states.

In order to solve the problem, we use one celebrated method to deal with many-body 1D problems: Matrix Product States (MPS).[54–56] Let us summarise the idea behind this technique. A general state of a many-body system is usually written as

$$|\Psi\rangle = \sum_{i_1,\ldots,i_{N_{\text{cav}}}} c_{i_1,\ldots,i_{N_{\text{cav}}}} |i_1,\ldots,i_{N_{\text{cav}}}\rangle, \tag{11}$$

where $\{|i_n\rangle\}_{i_n=1}^{d_n}$ is a basis of the local Hilbert space of the n-th body (or site, in our case), with d_n being the dimension of this local Hilbert space, $|i_1,\ldots,i_{N_{\text{cav}}}\rangle = |i_1\rangle\ldots|i_{N_{\text{cav}}}\rangle$, that is, the tensor product basis, and $c_{i_1,\ldots,i_{N_{\text{cav}}}} \in \mathbb{C}$. However, it is possible to show that an equivalent parametrisation can be written as:

$$|\Psi\rangle = \sum_{i_1,\ldots,i_{N_{\text{cav}}}} A_1^{i_1}\ldots A_{N_{\text{cav}}}^{i_{N_{\text{cav}}}} |i_1,\ldots,i_{N_{\text{cav}}}\rangle, \tag{12}$$

where $A_n^{i_n}$ is a $D_n \times D_{n+1}$ matrix linked to the n-th site.† For the sake of simplicity, let us take $d_n = d$ and $D_n = D$ for all n. Then, $N_{\text{cav}}D^2d$ coefficients are needed to describe any state. In principle, to represent $|\Psi\rangle$ exactly, D must be exponential in N_{cav}. However, states in the low energy sector of well-behaved many-body Hamiltonians can be very accurately described by taking D polynomial in N_{cav}.[57] Few photon dynamics belongs to this low energy sector and, as we will show, the number of MPS coefficients required to study scattering scales polynomially with N_{cav}. This technique has been recently applied to propagation in bosonic chains interacting with impurities.[46,48]

Our simulations are as follows: (i) initialisation of the state as $|0\rangle$, (ii) computation of the ground state by means of imaginary time evolution, using the Suzuki–Trotter decomposition[58] adapted to the MPS representation,[59] (iii) generation of the input state (eqn (5)), (iv) time evolution of the wave function up to $t = t_{\text{out}}$ (eqn (9)) again by means of Suzuki–Trotter decomposition and (v) computation of relevant quantities.

2.4 Observables and its computation with MPS

The time dependence of expected values,

$$\langle \mathscr{O}^t \rangle = \langle \Psi(t)|\mathscr{O}|\Psi(t)\rangle \tag{13}$$

where $\mathscr{O}$ is any Hermitian operator acting on waveguide, qubit variables or both, completely characterises the dynamics. Relevant values are the number of photons (in position and momentum spaces):

$$\langle n_x{}^t \rangle = \langle \Psi(t)|a_x^\dagger a_x|\Psi(t)\rangle \leftrightarrow \langle n_k{}^t \rangle = \frac{1}{L}\sum_{x_1x_2} e^{ik(x_1-x_2)} \left\langle \Psi(t)\middle|a_{x_1}^\dagger a_{x_2}\middle|\Psi(t)\right\rangle, \tag{14}$$

† We are taking open boundary conditions, so $D_{N_{\text{cav}}+1} = D_1 = 1$.

Published on 18 November 2014. Downloaded by UNIVERSIDAD DE ZARAGOZA on 11/06/2015 13:47:58.

or the qubit populations and correlations:

$$P_i^t = \langle \Psi(t)|\sigma_i^+\sigma_i^-|\Psi(t)\rangle,\ \langle \sigma_i^+\sigma_j^-\rangle = \langle \Psi(t)|\sigma_i^+\sigma_j^-|\Psi(t)\rangle. \tag{15}$$

Thus, for example, transmission and reflection coefficients can be obtained as

$$T_k = \langle {n_k}^{t_{\text{out}}}\rangle / \langle n_k^0\rangle, \quad R_k = \langle {n_{-k}}^{t_{\text{out}}}\rangle / \langle n_k^0\rangle. \tag{16}$$

The projectors

$$\phi^t_{x_1,\ldots,x_N} = \frac{1}{\sqrt{N!}}\langle \text{GS}|a_{x_1}\ldots a_{x_N}|\Psi(t)\rangle, \tag{17}$$

are fundamental, since, setting $t = t_{\text{out}}$ they are nothing but the Fourier transform of the scattering matrix $S_{p_1\ldots p_{N'},k_1\ldots k_N}$, eqn (10).

Let us start by considering an operator that can be expressed as product of local operators:

$$\mathcal{O} = o_1 o_2 \ldots o_{N_{\text{cav}}} \tag{18}$$

e.g. $O = a^\dagger_{x_i} a_{x_j}$ or $O = \sigma_j^- a_{xj}$. For the states $|\Psi_A\rangle$ and $|\Psi_B\rangle$, characterised by the tensors $\{A_n{}^{i_n}\}_{n=1}^{N_{\text{cav}}}$ and $\{B_n{}^{i_n}\}_{n=1}^{N_{\text{cav}}}$ respectively [*cf.* eqn (12)] the matrix element $\langle \Psi_A|\mathcal{O}|\Psi_B\rangle$ is given by

$$\langle \Psi_A|\mathcal{O}|\Psi_B\rangle = \prod_{n=1}^{N_{\text{cav}}} E_n(A_n, B_n, o_n), \tag{19}$$

with

$$E_n(A_n, B_n, o_n) = \sum_{i_n, j_n} \langle i_n|o_n|j_n\rangle \left(\left(A_n{}^{i_n}\right)^* \otimes B_n{}^{i_n} \right) \tag{20}$$

Since any operator can always be written as a sum of products of local operators, we can compute any expected value (13) and projector (17) without the explicit computation of the $c_{i_1,\ldots,i_{N_{\text{cav}}}}$ coefficients in eqn (11).

Let us specify the concrete MPS formulas for the relevant observables. If we are interested in the photon number, $\langle n_x{}^t\rangle$ (14), we compute (19) with $|\Psi_A\rangle = |\Psi_B\rangle = |\Psi(t)\rangle$, $o_x = a_x^\dagger a_x$, and $o_n = \mathbb{I}_n$ for $n \neq x_i$, with $\mathbb{I}_n$ the identity operator. In the same way, for $P_i{}^t$ defined in (15) we must replace $o_{xi} = \sigma_i^+\sigma_i^-$ and $o_n = \mathbb{I}_n$ for $n \neq x_i$. The momentum occupation number, $\langle n_k{}^t\rangle$ in (14) is computationally harder to obtain. We must compute every two-body operator $\langle a^\dagger_{x_1} a_{x_2}\rangle$ by taking $o_{x_1} = a^\dagger_{x_1}$, $o_{x2} = a_{x2}$ and $o_n = \mathbb{I}_n$ for $n \neq x_1, x_2$, with $|\Psi_A\rangle = |\Psi_B\rangle = |\Psi(t)\rangle$ and perform the sum in (14). We can also obtain two-body qubit correlators, $\sigma_i^+\sigma_j^-$, taking $o_{xi} = \sigma_i^+$, $o_{xj} = \sigma_j^-$ and $o_n = \mathbb{I}_n$ for $n \neq x_i, x_j$. Finally, for the projectors $\phi_{x_1,\ldots,x_N}{}^t$, eqn (17), one just takes $|\Psi_A\rangle = |\text{GS}\rangle$, $|\Psi_B\rangle = |\Psi(t)\rangle$, $o_{xi} = a_{xi}$ with $i = 1,\ldots,N$ and $o_n = \mathbb{I}_n$ for $n \neq x_1,\ldots,x_N$.

3 Linear scattering

The main objective of this work is to realise how nonlinear the scattering of few photons through few qubits is. To accomplish this task we need first to know what linear scattering is. In this section we discuss in general what we understand for

Published on 18 November 2014. Downloaded by UNIVERSIDAD DE ZARAGOZA on 11/06/2015 13:47:58.

linear quantum optics and its realisation in waveguide QED. Finally, we establish under which conditions a collection of qubits behave as a linear optical medium.

3.1 Linear systems

In quantum physics, linear systems are those whose Heisenberg equations for the observables form a linear set. For the case of Hamiltonian (1) this happens whenever the scatterers are harmonic resonators (the waveguide itself is linear) both within RWA and non-RWA coupling regimes. In this case, the $c_j,c_j^\dagger$ operators in (1) are *bosonic* operators [*cf.* eqn (2)]:

$$[c_i,c_j^\dagger] = \delta_{ij} \tag{21}$$

and [*cf.* eqn (3)]:

$$h_i(c_i,c_i^\dagger) = \Delta_i c_i^\dagger c_i. \tag{22}$$

where Δ_i are the resonator frequencies.

3.2 Analytical properties for the *S*-matrix whit harmonic resonators as scatterers

Once we know what linear scattering means, we present our first result. An equivalent result was introduced by us in the ESI of ref. 48. We re-express it here in a more convenient way.

Theorem1 3.1. If the system is linear (in the sense of Section 3.1), the one-photon scattering matrix is given by:

$$\langle p|S|k\rangle = t_k\delta_{p,k} + r_k\delta_{p,-k}. \tag{23}$$

The apparent simplicity of theorem 3.1 requires some discussion. Firstly, photon creation is not possible. Second, eqn (23) fixes the actual form for the output states,

$$|\Psi_{\text{out}}\rangle = \sum_{k>0}\left(t_k\phi_k^{\text{in}}a_k^\dagger + r_k\phi_k^{\text{in}}a_{-k}^\dagger\right)|\text{GS}\rangle. \tag{24}$$

Therefore, the only scattering processes for one incoming photon occurring within linear models are the reflection and transmission of the photon without changing its input energy (momentum). Notice that this is a non trivial feature, since the Hamiltonian (1) is not number conserving: $\left[H, \sum_x a_x^\dagger a_x + \sum_j c_j^\dagger c_j\right] \neq 0$ and the ground state $|\text{GS}\rangle$ does not have a well defined number of excitations. However, the single photon scatters by reflecting and transmitting without changing the energy and without creating additional excitations in the system. This result mathematically relies on the Bogolioubov transformation and physically on the fact that (1) is a free model in quantum field theory language. The proof of this theorem is found in Appendix A.

The single photon result, Theorem 3.1 can be generalised to the multiphoton case:

Theorem1 3.2. If the system is linear the *N*-photon scattering matrix is given by:

Published on 18 November 2014. Downloaded by UNIVERSIDAD DE ZARAGOZA on 11/06/2015 13:47:58.

$$\langle p_1, p_2, \ldots, p_N|S|k_1, k_2, \ldots, k_{N'}\rangle = \delta_{NN'} \sum_{n_1 \neq n_2 \neq \ldots \neq n_N} \langle p_1|S|k_{n_1}\rangle \ldots \langle p_N|S|k_{n_N}\rangle. \quad (25)$$

The theorem says that, in linear systems the scattering matrix is a product of single photon scattering matrices. Consequently, no particle creation, Raman processes or photon–photon interactions are possible. The proof, detailed in Appendix B, is based on the single photon result, Theorem 3.1, together with the Wick's theorem. To better appreciate these two general results, let us apply them.

3.3 The classical limit: recovering the standard linear optics concept

Theorems 3.1 and 3.2 dictate the scattering in linear systems (*i.e.*, when the scatterers are harmonic resonators). So far, it is not completely clear whether the definition for linear systems in quantum mechanics given in Section 3.1 (together with the results in Section 3.2) corresponds to what linear optics means: the properties for the scattered currents are independent of the input intensity. Here we show that linear systems satisfy this intensity independence. Importantly, we comment on the classical limit for linear systems.

We consider a monochromatic coherent state as the N-photon input state,

$$|\Psi_{\text{in}}\rangle = |\alpha_k\rangle = \mathrm{e}^{-|\alpha_k|^2/2} \sum_{n=0}^{\infty} \frac{{\alpha_k}^n \left(a_k^\dagger\right)^n}{n!} |\text{GS}\rangle. \quad (26)$$

Applying the theorems 3.1 and 3.2 the output state can be written as,

$$|\Psi_{\text{out}}\rangle = \mathrm{e}^{-|\alpha_k|^2/2} \sum_{n=0}^{\infty} \frac{{\alpha_k}^n \left(t_k a_k^\dagger + r_k a_{-k}^\dagger\right)^n}{n!} |\text{GS}\rangle = |t_k\alpha_k\rangle \otimes |r_k\alpha_{-k}\rangle. \quad (27)$$

The second equality follows after some algebra.‡

Eqn (27) is a satisfactory result. The transmission and reflection coefficients t_k and r_k are independent of α_k. Recalling that $\langle\alpha_k|a_k^\dagger a_k|\alpha_k\rangle = |\alpha_k|^2$, this means independence from input intensity. We note that linear systems transform coherent states onto coherent states. Thus harmonic resonators neither change the statistics nor generate entanglement between the reflected and transmitted fields. Coherent states can be considered as classical inputs in the limit $\alpha_k \to \infty$, thus linear systems do not generate quantumness. Finally, the last expression for $|\Psi_{\text{out}}\rangle$ in (27) has a classical interpretation in terms of transmitted $|t_k\alpha_k|^2$ and reflected $|r_k\alpha_k|^2$ currents ($|t_k|^2 + |r_k|^2 = 1$).

3.4 From nonlinear to linear

Consider M qubits placed at the same point of the waveguide, $x_i = x_j$ for all i, j in Hamiltonian (1). For simplicity, assume that the couplings g_i are also the same. Introducing the operator,

‡ Note that: $\sum_{n=0}^{\infty} \frac{\alpha_k{}^n (a_k^\dagger(t_{\text{out}}))^n}{n!} = \sum_{n=0}^{\infty}\sum_{m=0}^{n} \frac{1}{m!(n-m)!} (t_k\alpha_k a_k^\dagger)^m (r_k\alpha_k a_{-k}^\dagger)^{n-m}$

$= \sum_{n=0}^{\infty} \frac{\left(t_k\alpha_k a_k^\dagger\right)^n}{n!} \sum_{n'=0}^{\infty} \frac{\left(r_k\alpha_k a_{-k}^\dagger\right)^{n'}}{n'!}$

.

Published on 18 November 2014. Downloaded by UNIVERSIDAD DE ZARAGOZA on 11/06/2015 13:47:58.

$$b \equiv \frac{1}{\sqrt{M}} \sum_{i=1}^{M} \sigma_i^- , \tag{28}$$

the total Hamiltonian, eqn (1), can be rewritten as

$$H_{\mathrm{tot}} = \varepsilon \sum_x a_x^\dagger a_x - J \sum_x \left(a_x^\dagger a_{x+1} + \mathrm{hc}\right) + \Delta b^\dagger b + g\sqrt{M}\left(b^\dagger + b\right)\left(a_0^\dagger + a_0\right). \tag{29}$$

Thus, in terms of the Dicke states generated by (28) the effective coupling is $g\sqrt{M}$. Additionally, it is crucial to observe that[60]

$$\left[b, b^\dagger\right] = 1 - \frac{1}{M} \sum_j \sigma_j^+ \sigma_j^- \tag{30}$$

Therefore, in the limit $\left\langle \sum_j \sigma_j^+ \sigma_j^- \right\rangle / M \ll 1$ (a weak probe compared to the number of qubits) the operator b ($b^\dagger$) approximates an annihilation (creation) bosonic operator. Therefore, a large number of qubits is expected to behave as a harmonic resonator.

4 Nonlinear scattering: numerics in the RWA

We are interested in the nonlinear optical properties of a collection of qubits. The nonlinearities can be manifested in different observables. The theoretical results in Section 3.2 say nothing about the nonlinear regime. In the following, we will compute some natural quantities as the reflection and transmission probabilities or photon–photon correlation. We will evaluate how nonlinear the response is as a function of the number of incoming photons, number of qubits or inter qubit distance. Throughout this section the RWA is assumed. Physics beyond the RWA is discussed in the next section.

4.1 *N* photons *vs.* *M* qubits: total reflection spectrum

The combination of energy and number conservation implies that output states for one photon scattering through qubits in the RWA are also given by eqn (24) (like in linear systems). A well known result in this geometry is that a single monochromatic photon suffers perfect reflection, $|r_{k_{\mathrm{in}}}|^2 = 1$, when its frequency $\omega_{\mathrm{in}} = \Delta$;[61–63] this effect has several useful applications.[13,64–67] For linear systems, following (25), the N-photon S matrix is a product of single photon S matrices. Thus, in linear systems, N-photon input states must also be perfectly reflected at resonance. On the other hand, a qubit cannot totally reflect more than one photon at the same time.[17] Then, for N-photon ($N > 1$) input states perfect reflection is not expected to occur with one qubit. If we want to overpass this saturation effect, we may increase the number of qubits. In the limit $N/M \ll 1$, with N photons and M the number of qubits the linear regime should be recovered, *i.e.* perfect reflection should happen [see Section 3.4].

Equipped with the MPS technique we can study the linear–nonlinear transition as a function of the ratio N/M. In doing so, we provide meaning to the inequality $N/M \ll 1$. In this subsection we consider that the M qubits are placed at

Published on 18 November 2014. Downloaded by UNIVERSIDAD DE ZARAGOZA on 11/06/2015 13:47:58.

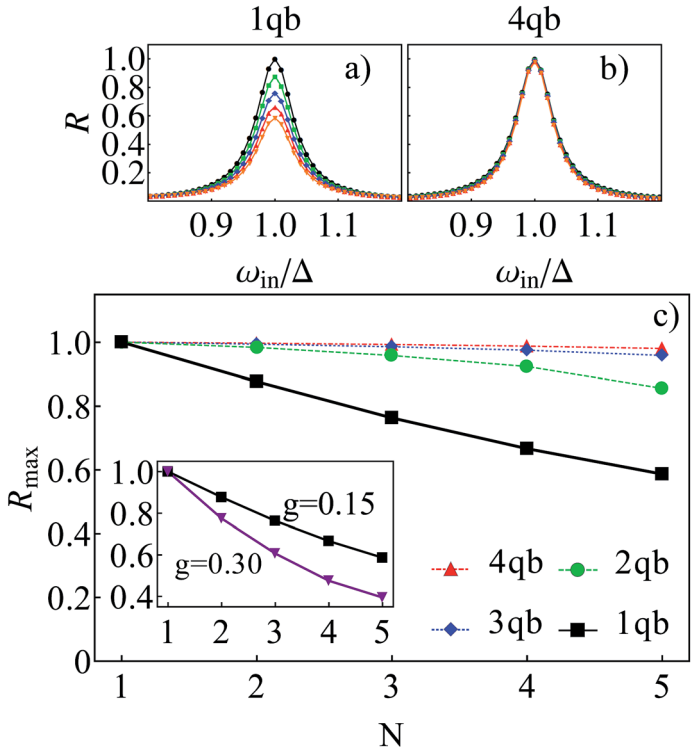

Fig. 2 ε, J and Δ are as in Fig. 1. The input state, eqn (5) and (6), with $k_{in} = \pi/2$ and $\theta = 2$. (a) R for $M = 1$ and $N = 1$–5 (black circles, green squares, blue diamonds, red triangles and orange inverted triangles respectively); (b) the same as in a) but with $M = 4$; (c) R_{max} for $g\sqrt{M} = 0.15$, with $M = 1$–5 qubits (black squares/solid line, green circles/dashed line, blue diamonds/dotted line and red triangles/dotted-dashed line respectively). In the inset we show R_{max} *vs.* N for $M = 1$, with $g = 0.15$ (black squares) and $g = 0.30$ (purple inverted triangles).

the same point, *i.e.*, their inter distance is zero. We compute $R_{\omega_{in}}$ from $N = 1$ to $N = 5$ photons input states given by (5) and (6) centred in the resonant value $k_{in} = \pi/2$ ($\omega_{k_{in}} = \Delta$). The scattering centre is composed by $M = 1$ to $M = 4$ qubits. We plot $R_{\omega_{in}}$ [*cf.* eqn (16)] for $M = 1$ and $M = 4$ qubits in Fig. 2(a and b) respectively. The spectral width scales with the one-photon effective coupling $g\sqrt{M}$ (29), which is maintained as constant in the calculations. As shown, the maximum reflection $R_{max} < 1$ as soon as $N > 1$. The effect is better observed in the $M = 1$ qubit case, as shown in Fig. 2(a). As argued before, by increasing the number of qubits we recover the full reflection $R_{max} \cong 1$. The dependence of R_{max} as a function of N/M is better represented in panel Fig. 2(c). R_{max} decreases much faster with N for $M = 1$ than for $M > 1$. For $M = 4$, R_{max} hardly gets modified by changing the number of photons in the considered range of N. Following refs 18 and 29 there is total reflection for $N = 2$ *vs.* $M = 2$ if the photon energies individually match with those of the qubits. We see a slight deviation from this result because we are taking a non-monochromatic input state and the component of the incident wavefunction for k_1, $k_2 \neq k_{in}$ is not negligible. It is remarkable that R_{max} does not only depend

Published on 18 November 2014. Downloaded by UNIVERSIDAD DE ZARAGOZA on 11/06/2015 13:47:58.

on N and M, but also on the coupling, see the inset in Fig. 2(c). Therefore the nonlinear characteristics do not only depend on the material (qubits) but on their coupling to the field too.

4.2 Two photons *vs.* M qubits: spatial photon–photon correlations in reflection

In this section we compute the photon–photon correlations created in the scattering process for two-photon input states, as a function of the number of qubits. For further comparison and understanding, we begin by discussing the linear case. In this case the scatterer is a harmonic oscillator $h = \Delta c^\dagger c$ with $[c, c^\dagger] = 1$ in eqn (1). It has already been discussed in this paper that no correlations are generated if the scatterer is linear [*cf.* Theorem 3.2]. The two point correlation factorises: $\left|\phi_{x_1,x_2}{}^{t_{\text{out}}}\right|^2 = \left|\phi_{x_1}{}^{t_{\text{out}}}\right|^2 \left|\phi_{x_2}{}^{t_{\text{out}}}\right|^2$ and, in particular, the two photons must be bunched both in reflection and transmission: $\left|\phi_{x,x}{}^{t_{\text{out}}}\right|^2 = \left|\phi_{x}{}^{t_{\text{out}}}\right|^4$. In the nonlinear case, however, the reflected field by one qubit is totally antibunched,[17] $\left|\phi_{x,x}{}^{t_{\text{out}}}\right|^2 = 0$. Thus, antibunching can be used as a witness for nonlinearities. With these antecedents, we provide answers to the following questions below. How does this depend on the number of qubits? Is it possible to interpolate between the highly nonlinear case of one qubit and the linear case of a harmonic oscillator by adding qubits? If so, how many qubits are needed for the system to be linear?

In Fig. 3d we plot the reflected $|\phi_{x_1,x_2}|^2$ against $x_1 - x_2$, fixing $(x_1 + x_2)/2$ such that the reflection component is maximum. The one-photon coupling, $g\sqrt{M}$ is kept constant for different M and equals the coupling g for the case of the harmonic oscillator. We remember that $|\phi_{x_1,x_2}|^2$ is proportional to the probability of having both photons separated by a distance $|x_1 - x_2|$. Setting $x_1 = x_2$ gives the probability of seeing both photons at the same point. For $M = 1$ the numerical results (Fig. 3d) show $|\phi_{xx}|^2 \simeq 0$, recovering the well known photon antibunching in reflection.[17,18] Surprisingly, photon antibunching and thus nonlinearity can still be resolved by increasing M, even for $M = 20$.§ The full contour for $|\phi_{x_1,x_2}|^2$ is shown in Fig. 3a–c for one and two qubits and a harmonic resonator respectively. Apart from the antibunched characteristics in the reflected signal, we can also appreciate that one qubit cannot reflect as much as two qubits, as we discussed in Section 4.1 [*cf.* Fig. 2]. The transmitted photons are always bunched. The components around $(x_1 + x_2)/2 \simeq 0$ and $|x_1 - x_2| \simeq 200$ correspond to one photon being transmitted and the other reflected.

Once the physics has been discussed, let us finish with a brief note on how to solve the two photon scattering against M qubits, for any M, placed at the same point and within the RWA. We start by remembering that the RWA implies the conservation for the number of excitations, *cf.* Section 2.1.

§ We note here that for the particular set of values $N = 2$ and $M = 2$ that, if $\omega_1 = \Delta_1$ and $\omega_2 = \Delta_2$ photons are bunched[18,29] as it would be linear scattering. However, our initial wavepacket is not monochromatic.

Published on 18 November 2014. Downloaded by UNIVERSIDAD DE ZARAGOZA on 11/06/2015 13:47:58.

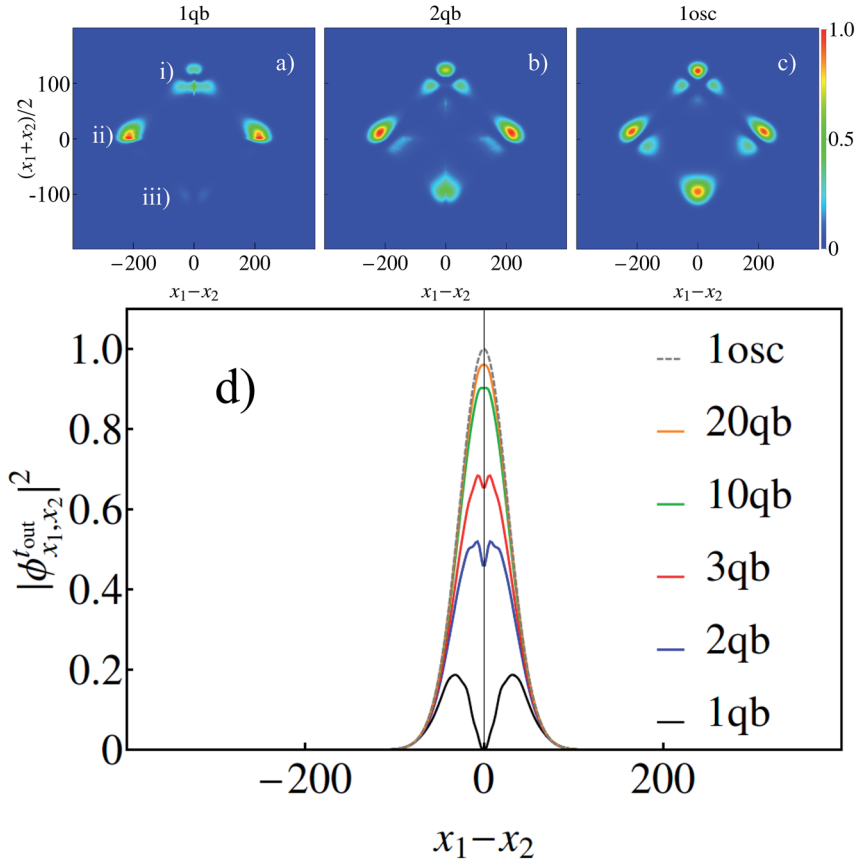

Fig. 3 $\left|\phi_{x_1,x_2}{}^{t_{out}}\right|^2$ for $g\sqrt{M} = 0.10$, with (a) $M = 1$ qubit, (b) $M = 2$ qubits and (c) a harmonic oscillator. $\left|\phi_{x_1,x_2}{}^{t_{out}}\right|^2$ is normalised in each panel such that its maximum is set to 1. In the contours, (i) corresponds to the transmitted–transmitted component, (ii) to the transmitted–reflected component and finally (iii) to the reflected–reflected component. (d) $\left|\phi_{x_1,x_2}{}^{t_{out}}\right|^2$ fixing $(x_1 + x_2)/2$ for $g\sqrt{M} = 0.10$, with $M = 1$, 2, 3, 10 and 20 qubits (solid, from bottom to top) and a harmonic oscillator (dashed). We normalise such that the correlator for the harmonic oscillator is 1 for $x_1 = x_2$. The input state is a 2-photon state with $k_{in} = \pi/2$ and $\theta = 20$.

Therefore, in the two excitation manifold and regarding the qubits, it will suffice to consider the following Dicke states: $\left\{|0\rangle, |1\rangle \equiv b^\dagger|0\rangle, |2\rangle \equiv \frac{(b^\dagger)^2|0\rangle}{\sqrt{2(1-1/M)}}\right\}$ [*cf.* eqn (28)]. Thus, if $N = 2$, the M qubits can be formally replaced by a three level system with states given as above. As expected [see Section 3.4], in the limit $M \to \infty$, $|2\rangle = \frac{(b^\dagger)^2|0\rangle}{\sqrt{2}}$ as in the harmonic oscillator case.

4.3 Three qubits with distance

We incorporate a new ingredient here, the inter-qubit distance. Interactions among qubits are mediated by the EM field decay with the distance in two and

Published on 18 November 2014. Downloaded by UNIVERSIDAD DE ZARAGOZA on 11/06/2015 13:47:58.

three dimensions.[68] One dimension is special: the field wavefront area does not grow with distance and, thus, the interaction does not decay but it is periodically modulated instead. The period depends on the qubits level splitting and the dispersion relation in the waveguide. This peculiarity has been theoretically investigated for qubits in a multitude of arrangements[34–37,69] and experimentally demonstrated quite recently.[7] For our purposes it is important to note that these works considered either classical or single photon input states. Two photon input states were considered too in refs 26 and 27.

Invoking the Markovian approximation the induced qubit–qubit interaction is considered instantaneous. This implies that the set of distances, $d \equiv x_{i'} - x_i$, related by

$$d' = d + \frac{\pi}{k_{\text{in}}} q, \quad q \in \mathbb{Z} \tag{31}$$

give the same scattering characteristics.

Let us consider $N = 2$ input photon states and three qubits separated by some nearest neighbour distance d. With the MPS tool, we solve the problem exactly, no matter the distance. Thus, we do not make any approximations, such as the small

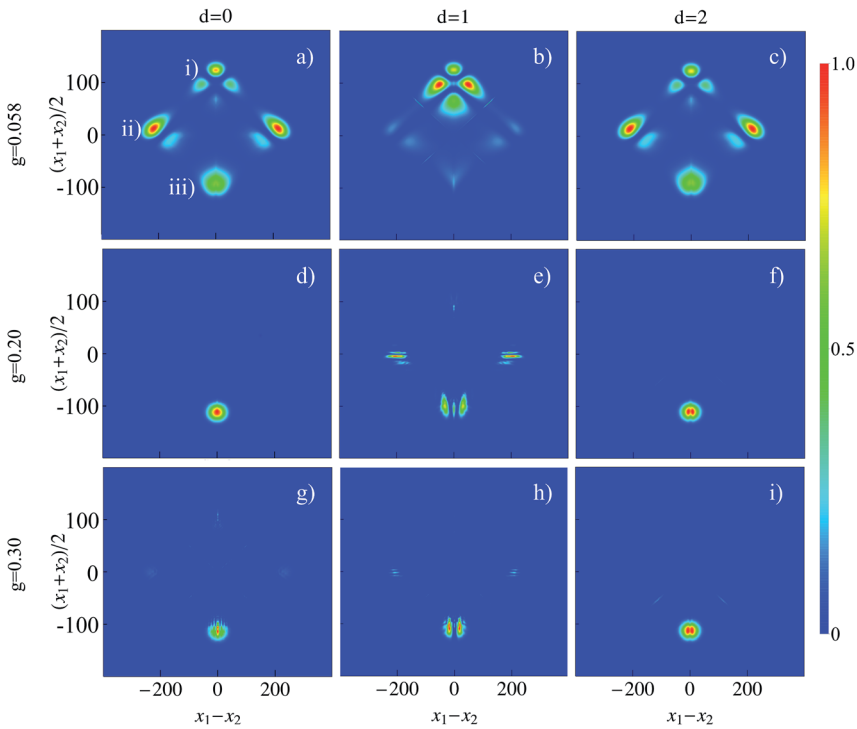

Fig. 4 $\left|\phi_{x_1,x_2}{}^{t_{\text{out}}}\right|^2$ for two incident photons and three qubits with inter-qubit distance d. (i–iii) mean the same as in Fig. 3. The incoming photons are characterised by $\theta = 20$ and $k_{\text{in}} = \pi/2$. We take $d = 0$, 1, 2 (left, middle and right columns respectively), so the first and the third cases should be equivalent because of (31). We consider the RWA Hamiltonian and take $g\sqrt{3} = 0.10$ in the first row, whereas we take the full Hamiltonian for the second and third rows, with $g = 0.20$ and $g = 0.30$ respectively.

 This journal is © The Royal Society of Chemistry 2015

Published on 18 November 2014. Downloaded by UNIVERSIDAD DE ZARAGOZA on 11/06/2015 13:47:58.

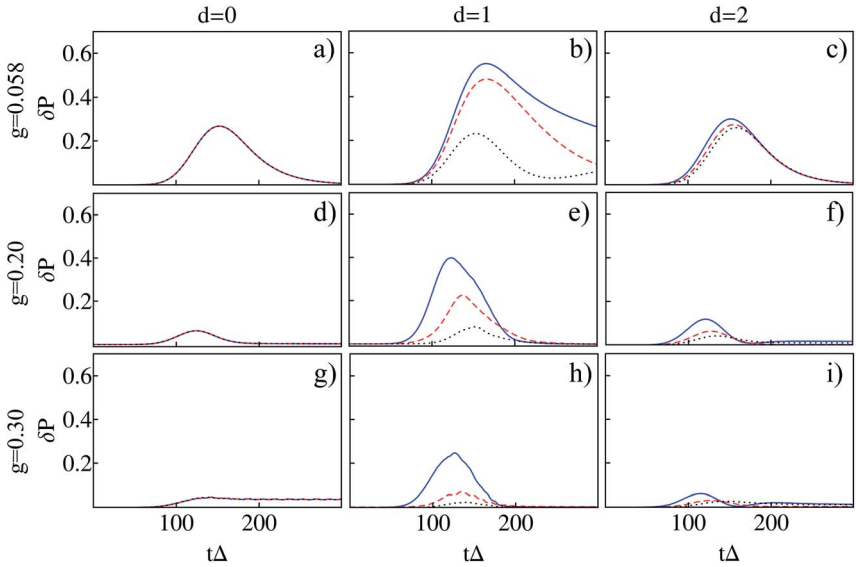

Fig. 5 Time evolution for the qubit population of the first (solid blue), the second (dashed red) and the third qubit (dotted black). The parameters are those of Fig. 4.

distance or Markovian approximations. We plot photon–photon correlations $\left|\phi_{x_1,x_2}{}^{t_{\text{out}}}\right|^2$ (17) and qubit populations $\delta P_i \equiv P_i - (P_i)_{\text{GS}}$ (15) for RWA couplings ($(P_i)_{\text{GS}} = 0$) in Fig. 4 and 5, panels (a–c) in both cases. Regarding the photons, the characteristics are the same at zero distance and $d = 2$, which is equivalent to zero distance, by means of (31) ($k_{\text{in}} = \pi/2$). On the other hand, the inherent non-Markovian properties of our exact simulation can be appreciated by comparing Fig. 5(a and c). If $d \neq 0$, the qubit at the left is excited first, then the central qubit and finally the one to the right.

The contours for the two-photon wave function $\left|\phi_{x_1,x_2}{}^{t_{\text{out}}}\right|^2$ are closer to the linear scattering result for $d = 0$ and $d = 2$ than those for the $d = 1$ case [*cf.* Fig. 3c and 4(a–c)]. This enhancement of nonlinear properties with the distance can be understood as follows. At distances $\frac{\pi}{k_{\text{in}}} q$, [equivalent to zero distance according to eqn (31)], only qubit states generated by the ladder operator b in eqn (28) are visited during the dynamics. For two photon input states, the nonlinearities die out as $1/M$ [*cf.* Section 4.2]. On the other hand, for other distances not fulfilling this condition of equivalence, more qubit states (satisfying the number conservation imposed by the RWA) can play a role. The fact that more qubit modes participate in the dynamics for $d = 1$ is apparent from Fig. 5(b). Clearly, more frequencies are involved in the evolution of P. Importantly enough, $d = 1$ corresponds to a distance where the coherent interaction between the qubits are maximised, while the correlations in the qubit decays are minimised. This is named as the subradiant case, as we can observe that the qubit decay (after excitation) is slower in this case.

Published on 18 November 2014. Downloaded by UNIVERSIDAD DE ZARAGOZA on 11/06/2015 13:47:58.

5 Nonlinear scattering in the ultrastrong regime

We close this discussions by investigating stronger qubit–photon couplings, strong enough to break down the RWA approximation, eqn (4). The full dipole interaction must be considered. When moving to the ultrastrong regime, the problem becomes rather involved. The ground state, $|\mathrm{GS}\rangle$, for (1) is not trivial anymore but strongly correlated and the number of excitations is not conserved [recall Section 2.1]. This increase in the complexity brings a lot of new phenomena. We fix our attention on two characteristics. First, we discuss the appearance of inelastic scattering at high couplings.[48,70–72] Second, we revisit the qubit–qubit interactions mediated by the guide in the ultrastrong coupling regime.

5.1 Inelastic scattering with M qubits

So far, we have discussed elastic scattering. In linear systems, this is the only possible process. When the scatterers are qubits, however, inelastic processes may happen.[48,70–72] In an inelastic process, the photons can excite localised light–matter states. Those localised states, eigenstates for the total Hamiltonian, remain excited after the photons pass through. By energy conservation it is clear that the outgoing photons must have less energy. Within the RWA approximation,[70–72] at least two photons are needed for inelastic processes. When the actual full dipole interaction is considered (1), a non stimulated Raman scattering process occurs.[48] Indeed, it is quite remarkable that 100% efficiency can be achieved.[48]

We study the inelastic channel for one photon input states when interacting with M qubits placed at the same point. In Fig. 6 we plot the transmitted current in the inelastic channel,

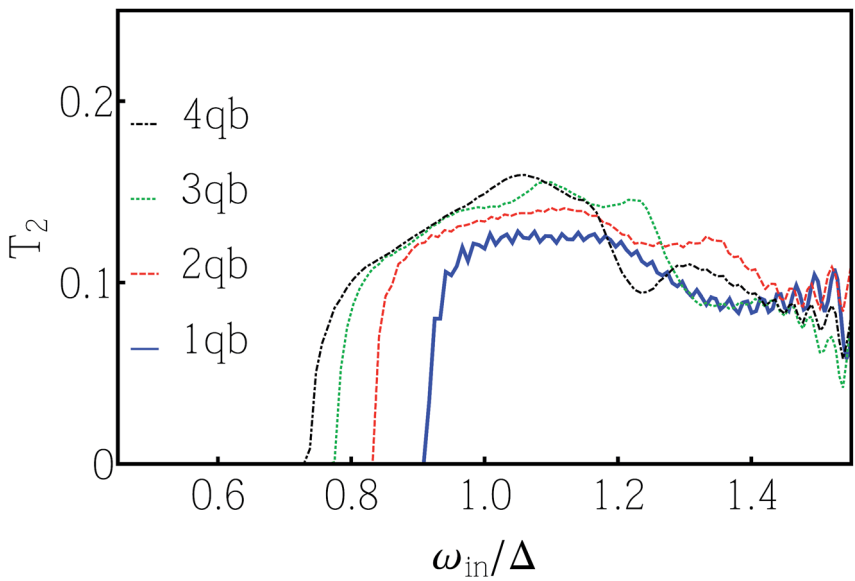

Fig. 6 Inelastic transmission probability for $g\sqrt{M} = 0.50$ and 1 qubit (solid blue), 2 qubits (dashed red), 3 qubits (dotted green) and 4 qubits (dashed-dotted black).

 This journal is © The Royal Society of Chemistry 2015

Published on 18 November 2014. Downloaded by UNIVERSIDAD DE ZARAGOZA on 11/06/2015 13:47:58.

$$T_{2,k} = \frac{1}{2}\left(1 - |t_k|^2 - |r_k|^2\right) \tag{32}$$

In the figure we consider the qubits placed in the same point. This figure shows that inelastic scattering is another nonlinear characteristic which persists even for $N \ll M$ (recall that T_2 for a linear system is always zero, *cf.* Section 3.1).

5.2 Mixing distance and the ultrastrong regime

Interesting physics occurs with spatially separated qubits, when their interactions are mediated through the photons. At the same time the photons interact among themselves when they pass through those qubits. In the weak coupling regime, the output field is periodic in the qubit–qubit distance when taking the Markovian approximation (31) [see Section 4.3]. Below, we discuss how this scenario changes in the ultrastrong coupling regime.

In Fig. 4 the loss of this effective periodicity in the qubit distance is clearly shown by plotting $\left|\phi_{x_1,x_2}{}^{t_{\text{out}}}\right|^2$. At weak coupling (first row, already discussed in Section 4.3) the distances $d = 0$ and $d = 2$ satisfying (31) present identical output fields. The two lower rows show results at larger couplings. The condition (31) does not hold anymore, and the dipole–dipole periodic structure paradigm for one dimensional systems[7,34–36,69] is no longer true. Further confirmation is obtained when looking to the qubit dynamics. In the final column, we realise that, in the ultrastrong regime, signatures of subradiant dynamics are still perceived. The loss of periodicity is also appreciated here. If we fix our attention to the $d = 0$ case all qubits behave in the same manner, as they must, and they remain in an excited state, which is a signature of inelastic scattering. For the case $d = 2$, which in weak coupling is equivalent to $d = 0$ [*cf.* eqn (31)], the dynamics is completely different (see Fig. 5). At this set of parameters the qubits seem to evolve back to the ground state. Therefore no inelastic scattering occurs in this case.

6 Conclusions

The advent of artificial devices (optical cavities, superconducting circuits, dielectric and plasmonic guides, photonic crystals) opens the avenue for stronger and stronger light–matter coupling (at the single photon level). Recent impressive experimental advances are changing the paradigm and typical nonlinear effects can be observed at the few photon level. From the theoretical point of view, both light and matter must be described quantum mechanically. Going beyond one or two photons and one qubit is an analytically titanic task. Therefore, numerical tools are demanded to satisfy current experimental efforts in constructing devices responding nonlinearly at minimum powers. In this discussion we have shown that the MPS technique developed for one dimensional systems is a powerful tool in few photon nonlinear optics.

On the physical side, our task was to study the nonlinear response by increasing the number of qubits. It has a practical motif. The effective coupling scales with $g\sqrt{M}$ (M the number of qubits). Adding scatterers is a way to enhance the coupling but, at the same time, their nonlinear response is reduced. Some quantities, as the transmitted and reflected currents, already gave linear

Published on 18 November 2014. Downloaded by UNIVERSIDAD DE ZARAGOZA on 11/06/2015 13:47:58.

behaviour for ratios $N/M \cong 1$. However, we have found that for $N = 2$ input states, $M = 20$ qubits still generate photon–photon interactions.

We have also investigated the regime where light and matter are coupled ultrastrongly. New phenomena appear as Raman scattering or the breakdown of the periodicity in the qubit–qubit interaction, which should be observable by current technology, since some experimental setups already operate in the ultrastrong coupling regime. All together, this serves as a motivation for developing theories for its understanding and hopefully, will trigger further experimental studies for verifying the plethora of new phenomenology.

A Proof of theorem 3.1

If the scatterers are harmonic resonators the Hamiltonian (1) is linear [*cf.* Section 3.1] and it can be diagonalised with a Bogolioubov–Valatin (BV) transformation,

$$H = \sum \Lambda_l \alpha_l^\dagger \alpha_l, \tag{33}$$

with $[\alpha_l, \alpha_m^\dagger] = \delta_{lm}$ and $\Lambda_l > 0 \forall l$. The ground state is $\alpha_l|\mathrm{GS}\rangle = 0 \forall l$. The BV transformation

$$\alpha_l = \sum_{i=-L}^{L} \left(\chi_{li}{}^a a_i + \eta_{li}{}^a a_i^\dagger\right) + \sum_{i=1}^{M} \left(\chi_{li}{}^c c_i + \eta_{li}{}^c c_i^\dagger\right) \tag{34}$$

is invertible.

Hamiltonian (33) commutes with $N_\alpha = \sum \alpha_l^\dagger \alpha_l$:

$$[H, N_\alpha] = 0. \tag{35}$$

The number of α-excitations, N_α, is a good quantum number. It also conserves parity, $P = \mathrm{e}^{i\pi \sum \alpha_l^\dagger \alpha_l}$:

$$[H, P] = 0. \tag{36}$$

Single photon input states, $N = 1$ in (5), are written in momentum space

$$|\Psi_{\mathrm{in}}\rangle = \sum_{k>0} \tilde{\phi}_k^{\mathrm{in}} a_k^\dagger |\mathrm{GS}\rangle, \tag{37}$$

with $\tilde{\phi}_k^{\mathrm{in}}$ the Fourier transform of ϕ_x^{in}. Using the transformation (34) and that $\alpha_l|\mathrm{GS}\rangle = 0$, we can rewrite the state (37) in the α-representation

$$|\Psi_{\mathrm{in}}\rangle = \sum_l \overline{\phi}_l^{\mathrm{in}} \alpha_l^\dagger |\mathrm{GS}\rangle. \tag{38}$$

Given the input state (38): $N_\alpha|\Psi_{\mathrm{in}}\rangle = |\Psi_{\mathrm{in}}\rangle$. Since N_α is a conserved quantity [*cf.* eqn (35)] the time evolution is restricted to the one α-excitation level (35). The output state is then

$$|\Psi_{\mathrm{out}}\rangle = \sum_l \overline{\phi}_l^{\mathrm{out}} \alpha_l^\dagger |\mathrm{GS}\rangle, \tag{39}$$

with $\overline{\phi}_l^{\mathrm{out}} \equiv \mathrm{e}^{-i\Lambda_l t_{\mathrm{out}}} \overline{\phi}_l^{\mathrm{in}}$. Using the transformation (34), the output state is rewritten

 This journal is © The Royal Society of Chemistry 2015

Published on 18 November 2014. Downloaded by UNIVERSIDAD DE ZARAGOZA on 11/06/2015 13:47:58.

$$|\Psi_{out}\rangle = \sum_l \overline{\phi}_l^{\text{out}} \left(\sum_k \left(\left(\tilde{\chi}_{lk}{}^a\right)^* a_k^\dagger + \left(\tilde{\eta}_{lk}{}^a\right)^* a_k \right) + \sum_i \left(\left(\chi_{li}{}^c\right)^* c_i^\dagger + \left(\eta_{li}{}^c\right)^* c_i \right) \right) |\text{GS}\rangle, \tag{40}$$

with $\tilde{\chi}_{lk}{}^a$ and $\tilde{\eta}_{lk}{}^a$ the discrete Fourier transforms of $\tilde{\chi}_{li}{}^a$ and $\tilde{\eta}_{li}{}^a$ in the second index. The output state (40) removes the possibility of having multiphoton scattering states. Therefore, the scattering events can be elastic, with transmission and reflection amplitudes t_k and r_k and inelastic, with the scatterer relaxing to an excited state $|\text{EXC}\rangle$. In the latter, the photon emerges with a new momentum k_{new}, fulfilling energy conservation

$$\omega_{k_{\text{in}}} + E_{\text{GS}} = \omega_{k_{\text{new}}} + E_{\text{EXC}} \tag{41}$$

Therefore, the output state can be rewritten

$$|\Psi_{\text{out}}\rangle = \sum_{k>0} \tilde{\phi}_k^{\text{in}} \left(t_k a_k^\dagger + r_k a_{-k}^\dagger \right) |\text{GS}\rangle + \sum_k \tilde{\phi}_k^{\text{new}} a_k^\dagger |\text{EXC}\rangle, \tag{42}$$

with $\tilde{\phi}_k^{\text{new}}$ a wavepacket centred around k_{new}.

Let us fix our attention to the second term in the r.h.s. of (42), which is rewritten in terms of the α-operators with the help of the BV transformation (34):

$$\sum_k \tilde{\phi}_k^{\text{new}} a_k^\dagger |\text{EXC}\rangle = \sum_l \left(\overline{\phi}_l{}^{\text{new},p} \alpha_l^\dagger + \overline{\phi}_l{}^{\text{new},m} \alpha_l \right) |\text{EXC}\rangle \tag{43}$$

Using N_α and P conservation, eqn (35) and (36), $N_\alpha |\text{EXC}\rangle = 2n|\text{EXC}\rangle$ with $n \geq 1$. The first term in the r.h.s. of (43) has $2n+1 \geq 3$ particles. Thus, $\bar{\phi}_l^{\text{new},p} = 0$. Finally $\alpha_l|\text{EXC}\rangle$ is an eigenstate of (33) with eigen-energy $E_{\text{EXC}} - \Lambda_l$ ($\Lambda_l > 0$). The latter must be equal to $\omega_{k_{\text{new}}} + E_{\text{EXC}}$ which is impossible. Therefore $\bar{\phi}_l^{\text{new},m} = 0$.

Putting this all together, the output state contains only the elastic channel,

$$|\Psi_{\text{out}}\rangle = \sum_{k>0} \tilde{\phi}_k^{\text{in}} \left(t_k a_k^\dagger + r_k a_{-k}^\dagger \right) |\text{GS}\rangle. \tag{44}$$

This ends the proof.

B Proof of theorem 3.2

The components for the scattering matrix (10) can be rewritten,

$$S_{p_1 \ldots p_{N'}, k_1 \ldots k_N} = \langle \text{GS} | a_{p_1} \ldots a_{p_{N'}} a_{k_1}^\dagger(t_{\text{out}}) \ldots a_{k_N}^\dagger(t_{\text{out}}) | \text{GS} \rangle \tag{45}$$

with

$$a_k^\dagger(t_{\text{out}}) = S^\dagger a_k^\dagger S = \left(t_k a_k^\dagger + r_k a_{-k}^\dagger \right). \tag{46}$$

In the last equality we have used (i) linearity: the Heisenberg evolution for the operators $a_{kn}(t)$ is independent of the input states, and (ii) the theorem 3.2. Eqn (46), together with the Wick theorem:

$$\langle \text{GS} | a_{p_1} \ldots a_{p_{N'}} a_{k_1}^\dagger \ldots a_{k_N}^\dagger | \text{GS} \rangle = \delta_{NN'} \sum_{m_1 \neq m_2 \neq \ldots \neq m_N} \delta_{p_1 k_{m_1}} \ldots \delta_{p_N k_{m_N}} \tag{47}$$

Published on 18 November 2014. Downloaded by UNIVERSIDAD DE ZARAGOZA on 11/06/2015 13:47:58.

completes the proof.

Acknowledgements

We acknowledge support by the Spanish Ministerio de Economia y Competitividad within projects MAT2011-28581-C02, FIS2012-33022 and No. FIS2011-25167, the Gobierno de Aragon (FENOL group) and the European project PROMISCE.

References

1 R. W. Boyd, *Nonlinear Optics*, Academic Press, 2nd edn, 2003.
2 T. Peyronel, O. Firstenberg, Q.-Y. Liang, S. Hofferberth, A. V. Gorshkov, T. Pohl, M. D. Lukin and V. Vuletic, *Nature*, 2012, **488**, 57.
3 O. Firstenberg, T. Peyronel, Q.-Y. Liang, A. V. Gorshkov, M. D. Lukin and V. Vuleti, *Nature*, 2013, **502**, 71.
4 J. Q. You and F. Nori, *Nature*, 2011, **474**, 589–597.
5 O. Astafiev, A. M. Zagoskin, A. A. Abdumalikov, Y. A. Pashkin, T. Yamamoto, K. Inomata, Y. Nakamura and J. S. Tsai, *Science*, 2010, **327**, 840.
6 I. C. Hoi, C. M. Wilson, G. Johansson, J. Lindkvist, B. Peropadre, T. Palomaki and P. Delsing, *New J. Phys.*, 2013, **15**, 025011.
7 A. F. van Loo, A. Fedorov, K. Lalumière, B. C. Sanders, A. Blais and A. Wallraff, *Science*, 2013, **342**, 1494.
8 T. Lund-Hansen, S. Stobbe, B. Julsgaard, H. Thyrrestrup, T. Sünner, M. Kamp, A. Forchel and P. Lodahl, *Phys. Rev. Lett.*, 2008, **101**, 113903.
9 J. L. O'Brien, *Science*, 2007, **318**, 1567.
10 Y. Rezus, S. Walt, R. Lettow, A. Renn, G. Zumofen, S. Gotzinge and V. Sandoghdar, *Phys. Rev. Lett.*, 2012, **108**, 093601.
11 R. W. Boyd, *Plasmonics: Fundamentals and Applications*, Springer, 2nd edn, 2007.
12 D. E. Chang, A. S. Sørensen, P. R. Hemmer and M. Lukin, *Phys. Rev. Lett.*, 2006, **97**, 053002.
13 A. V. Akimov, A. Mukherjee, C. L. Yu, D. E. Chang, A. S. Zibrov, P. R. Hemmer, H. Park and M. D. Lukin, *Nat. Phys.*, 2007, **450**, 402.
14 A. L. Falk, F. H. L. Koppens, C. L. Yu, K. Kang, N. de Leon Snapp, A. V. Akimov, M.-H. Jo, M. D. Lukin and H. Park, *Nat. Phys.*, 2009, **10**, 475.
15 N. P. de Leon, M. D. Lukin and H. Park, *IEEE J. Sel. Top. Quantum Electron.*, 2012, **18**, 1781.
16 J.-T. Shen and S. Fan, *Phys. Rev. A*, 2007, **76**, 062709.
17 J.-T. Chen and S. Fan, *Phys. Rev. Lett.*, 2007, **98**, 153003.
18 T. Shi, S. Fan and C. P. Sun, *Phys. Rev. A*, 2011, **84**, 063803.
19 E. Rephaeli, Ş. Kocabaş and S. Fan, *Phys. Rev. A*, 2011, **84**, 063832.
20 S. Xu, E. Rephaeli and S. Fan, *Phys. Rev. Lett.*, 2013, **111**, 223602.
21 T. Shi and C. P. Sun, *Phys. Rev. B: Condens. Matter Mater. Phys.*, 2009, **79**, 205111.
22 V. I. Yudson and P. Reineker, *Phys. Rev. A*, 2008, **78**, 052713.
23 H. Zheng, D. J. Gauthier and H. U. Baranger, *Phys. Rev. A*, 2010, **82**, 063816.
24 H. Zheng, D. J. Gauthier and H. U. Baranger, *Phys. Rev. Lett.*, 2011, **107**, 223601.
25 H. Zheng, D. J. Gauthier and H. U. Baranger, *Phys. Rev. A*, 2012, **85**, 043832.

 This journal is © The Royal Society of Chemistry 2015

Published on 18 November 2014. Downloaded by UNIVERSIDAD DE ZARAGOZA on 11/06/2015 13:47:58.

26 H. Zheng and H. U. Baranger, *Phys. Rev. Lett.*, 2013, **110**, 113601.
27 Y.-L. L. Fang, H. Zheng and H. U. Baranger, *EPJ Quantum Technol.*, 2014, **1**, 3.
28 D. Roy, *Phys. Rev. A*, 2011, **83**, 043823.
29 D. Roy, *Phys. Rev. A*, 2013, **87**, 063819.
30 J.-Q. Liao and C. K. Law, *Phys. Rev. A*, 2010, **82**, 053836.
31 B. Peropadre, J. Lindkvist, I. C. Hoi, C. M. Wilson, J. J. García-Ripoll, P. Delsing and G. Johansson, *New J. Phys.*, 2013, **15**, 035009.
32 E. Rephaeli and S. Fan, *Phys. Rev. Lett.*, 2012, **108**, 143602.
33 G.-Y. Chen, N. Lambert, C.-H. Chou, Y.-N. Chen and F. Nori, *Phys. Rev. B: Condens. Matter Mater. Phys.*, 2011, **84**, 045310.
34 A. González-Tudela, D. M. Cano, E. Moreno, L. Martín-Moreno, C. Tejedor and F. J. García-Vidal, *Phys. Rev. Lett.*, 2011, **106**, 020501.
35 D. Zueco, J. J. Mazo, E. Solano and J. J. García-Ripoll, *Phys. Rev. B: Condens. Matter Mater. Phys.*, 2012, **86**, 024503.
36 K. Lalumière, B. C. Sanders, A. F. van Loo, A. Fedorov, A. Wallraff and A. Blais, *Phys. Rev. A*, 2013, **88**, 043806.
37 C. González-Ballestero, E. Moreno and F. J. García-Vidal, *Phys. Rev. A*, 2014, **89**, 042328.
38 C. Cohen-Tannoudji, J. Dupont-Roc and G. Grynberg, *Atom-Photon Interactions: Basic Processes and Applications*, Wiley-Interscience, 1992, p. 680.
39 T. Niemczyk, F. Deppe, H. Huebl, E. Menzel, F. Hocke, M. Schwarz, J. J. García-Ripoll, D. Zueco, T. Hümmer, E. Solano, A. Marx and R. Gross, *Nat. Phys.*, 2010, **6**, 772.
40 P. Forn-Díaz, J. Lisenfeld, D. Marcos, J. J. García-Ripoll, E. Solano, C. J. P. M. Harmans and J. E. Mooij, *Phys. Rev. Lett.*, 2010, **105**, 237001.
41 T. Schwartz, J. A. Hutchinson, C. Genet and T. W. Ebbesen, *Phys. Rev. Lett.*, 2011, **106**, 196405.
42 G. Günter, A. A. Anappara, J. Hees, A. Sell, G. Biasol, L. Sorba, S. D. Liberato, C. Ciuti, A. Tredicucci, A. Leitenstorfer and R. Huber, *Nature*, 2009, **458**, 178.
43 S. De Liberato and C. Ciuti, *Phys. Rev. B: Condens. Matter Mater. Phys.*, 2008, **77**, 155321.
44 K. L. Hur, *Phys. Rev. B: Condens. Matter Mater. Phys.*, 2012, **85**, 140506.
45 G. Romero, D. Ballester, Y. M. Wang, V. Scarani and E. Solano, *Phys. Rev. Lett.*, 2012, **108**, 120501.
46 B. Peropadre, D. Zueco, D. Porras and J. J. García-Ripoll, *Phys. Rev. Lett.*, 2013, **111**, 243602.
47 U. Naether, J. J. García-Ripoll, J. J. Mazo and D. Zueco, *Phys. Rev. Lett.*, 2014, **112**, 074101.
48 E. Sánchez-Burillo, D. Zueco, J. J. García-Ripoll and L. Martín-Moreno, arXiv:1406.5779v1 [quant-ph], 2014.
49 Z. H. Wang, Y. Li, D. L. Zhou, C. P. Sun and P. Zhang, *Phys. Rev. A*, 2012, **86**, 023824.
50 R. H. Dicke, *Phys. Rev.*, 1954, **93**, 99.
51 D. Witthaut and A. S. Sørensen, *New J. Phys.*, 2010, **12**, 043052.
52 D. Roy, *Phys. Rev. Lett.*, 2011, **106**, 053601.
53 C. Cohen-Tannoudji, J. Dupont-Roc and G. Grynberg, *Photons & Atoms: Introduction to Quanutm Electrodynamics*, Wiley Vch, 1997, p. 486.
54 G. Vidal, *Phys. Rev. Lett.*, 2003, **91**, 147902.
55 G. Vidal, *Phys. Rev. Lett.*, 2004, **93**, 040502.

Published on 18 November 2014. Downloaded by UNIVERSIDAD DE ZARAGOZA on 11/06/2015 13:47:58.

56 F. Verstraete, V. Murg and J. I. Cirac, *Adv. Phys.*, 2008, **57**, 143.
57 J. Eisert, M. Cramer and M. B. Plenio, *Rev. Mod. Phys.*, 2010, **82**, 277–306.
58 M. Suzuki, *J. Math. Phys.*, 1991, **32**, 400.
59 J. J. García-Ripoll, *New J. Phys.*, 2006, **8**, 305.
60 T. Hümmer, G. Reuther, P. Hänggi and D. Zueco, *Phys. Rev. A*, 2012, **85**, 052320.
61 J.-T. Shen and S. Fan, *Opt. Lett.*, 2005, **30**, 2001.
62 J.-T. Shen and S. Fan, *Phys. Rev. Lett.*, 2005, **95**, 213001.
63 L. Zhou, Z. R. Gong, Y. xi Liu, C. P. Sun and F. Nori, *Phys. Rev. Lett.*, 2008, **101**, 100501.
64 L. Zhou, S. Yang, Y. xi Liu, C. P. Sun and F. Nori, *Phys. Rev. A*, 2009, **80**, 062109.
65 J.-Q. Liao, Z. R. Gong, L. Zhou, Y. xi Liu, C. P. Sun and F. Nori, *Phys. Rev. A*, 2010, **81**, 042304.
66 L. Zhou, L.-P. Yang, Y. Li and C. P. Sun, *Phys. Rev. Lett.*, 2013, **111**, 103604.
67 J. Lu, L. Zhou, L.-M. Kuang and F. Nori, *Phys. Rev. A*, 2014, **89**, 013805.
68 R. H. Lehmberg, *Phys. Rev. A*, 1970, **2**, 883.
69 L. Zhou, H. Dong, Y. xi Liu, C. P. Sun and F. Nori, *Phys. Rev. A*, 2008, **78**, 063827.
70 P. Longo, P. Schmitteckert and K. Busch, *Phys. Rev. Lett.*, 2010, **104**, 023602.
71 P. Longo, P. Schmitteckert and K. Busch, *Phys. Rev. A*, 2011, **83**, 063828.
72 T. Shi and C. P. Sun, arXiv:0907.2776 [quant-ph], 2009.

 This journal is © The Royal Society of Chemistry 2015